Two-stage Robust Optimization for Assessment of PV Hosting Capacity Based on Decision-dependent Uncertainty

Haifeng Qiu, *Senior Member, IEEE*, Veerapandiyan Veerasamy, *Member, IEEE*, Chao Ning, *Member, IEEE*, Qirun Sun, *Graduate Student Member, IEEE*, and Hoay Beng Gooi, *Fellow, IEEE*

Abstract—Photovoltaic (PV) generation always exhibits strong uncertainty and variability; therefore, its excessive integration brings huge risks to the safe operation of power systems. In this letter, a two-stage robust optimization approach based on decision-dependent uncertainty is devised to identify the PV hosting capacity that can be accepted to ensure the effective consumption of PV generation under uncertainty. The proposed approach is validated by numerical experiments for a microgrid and a distribution network.

Index Terms—Uncertainty, normalization, photovoltaic (PV) hosting capacity, robust optimization.

I. INTRODUCTION

WITH the rapid advancement of distributed generation technology, more photovoltaic (PV) and energy storage (ES) systems are integrated into power systems [1]. Nevertheless, PV generation cannot be precisely forecasted due to abrupt weather conditions, and its power uncertainty poses serious challenges to power system operation [2]. How to effectively identify the appropriate capacity of PV generation that can be accommodated is the primary problem that needs to be addressed for incorporating the integrated PV-ES systems into power systems [3].

To tackle this problem, research efforts have been devoted to the decision-making of PV hosting capacity [4]. Some studies resort to two-stage robust optimization (TSRO) approaches to evaluate the PV hosting capacity in power sys-

tems and ensure its secure operation under arbitrary PV output uncertain fluctuations [5]. Nonetheless, it is worth mentioning that the uncertainty of PV generation is directly associated with its configured capacity. Hence, TSRO for PV hosting capacity is essentially a class of decision-dependent uncertainty (DDU) based problems, which is usually ignored in existing studies. As the uncertainty set varies with endogenous decisions, the traditional decision-independent uncertainty (DIU) based algorithm suffers from the issue of iterative oscillation while solving DDU-based problems [6], resulting in the modeling computation not converging to the solution.

To fill the above research gap, this letter proposes a novel TSRO approach based on DDU involving both modeling and algorithm aspects for the assessment of PV hosting capacity in power systems. A normalization scheme is devised to equivalently reformulate the resulting DDU-based model as a regular TSRO model, which facilitates the efficient solution to this complicated optimization problem.

II. PROBLEM FORMULATION

The DDU-based TSRO model (M) for assessing the PV hosting capacity in power systems is developed in (1)-(19). The first-stage optimization maximizes the total PV hosting capacity ahead of uncertainty, and the second-stage model determines the feasible scheduling plans after realizations of source-load uncertainty under the corresponding capacity. In particular, the total power imbalance in the worst-case uncertainty scenario is minimized to be zero, i.e., the PV hosting capacity derived in the first stage shows guaranteed robustness.

$$\text{M:} \max_{\mathbf{x} = \left\{ C_i^{\text{PV}}, C_i^{\text{ES}}, M_i^{\text{ES+}}, M_i^{\text{ES-}} \right\}} \sum_{i=1}^{I} C_i^{\text{PV}} \tag{1}$$

s.t.

$$\begin{cases} C_i^{\text{ES}} = \alpha_i C_i^{\text{PV}} \\ M_i^{\text{ES+}} = \beta_i^+ C_i^{\text{ES}} \\ M_i^{\text{ES-}} = \beta_i^- C_i^{\text{ES}} \end{cases} \tag{2}$$

H. Qiu (corresponding author), V. Veerasamy, H. B. Gooi are with the School of Electrical and Electronic Engineering, Nanyang Technological University, Singapore 639798 (e-mail: hai-feng.qiu@ntu.edu.sg; veerapandiyan.v@ntu.edu.sg; ehbgooi@ntu.edu.sg).

C. Ning is with the Department of Automation, Shanghai Jiao Tong University, Shanghai 200240, China (e-mail: chao.ning@sjtu.edu.cn).

Q. Sun is with the School of Electrical Engineering, Southeast University, Nanjing 210096, China (e-mail: 230218326@seu.edu.cn).

$$\Phi = \max_{\boldsymbol{u} \in \Xi} \min_{\boldsymbol{y}^{\mathrm{b}}, \boldsymbol{y}^{\mathrm{c}}, \boldsymbol{\xi}} \sum_{t=1}^{T} \sum_{i=1}^{I} \left(\xi_{it}^{+} + \xi_{it}^{-} + \zeta_{it}^{+} + \zeta_{it}^{-} \right) \Rightarrow$$

$$\begin{cases} \boldsymbol{u} = \left\{ u_{it}^{\mathrm{PV}}, u_{it}^{\mathrm{LD}} \right\} \\ \boldsymbol{y}^{\mathrm{b}} = \left\{ z_{it}^{\mathrm{ES}+}, z_{it}^{\mathrm{ES}-}, z_{it}^{\mathrm{GL}+}, z_{it}^{\mathrm{GL}-} \right\} \\ \boldsymbol{y}^{\mathrm{c}} = \left\{ Q_{it}^{\mathrm{PV}}, P_{it}^{\mathrm{ES}+}, P_{it}^{\mathrm{ES}-}, Q_{it}^{\mathrm{ES}}, S_{it}, P_{it}^{\mathrm{GL}+}, P_{it}^{\mathrm{GL}-}, \right. \\ \qquad \left. Q_{it}^{\mathrm{GL}}, Q_{it}^{\mathrm{LD}}, P_{ijt}, Q_{ijt}, I_{ijt}, V_{it} \right\} \\ \boldsymbol{\xi} = \left\{ \xi_{it}^{+}, \xi_{it}^{-}, \zeta_{it}^{+}, \zeta_{it}^{-} \right\} \end{cases} \tag{3}$$

where x is the variable set of the first-stage optimization; C_i^{PV} and C_i^{ES} are the capacities of the PV and ES at node i, respectively; $M_i^{\mathrm{ES}+}$ and $M_i^{\mathrm{ES}-}$ are the maximal charging and discharging power of ES i, respectively; α_i is the capacity ratio of the integrated PV and ES system; β_i^+ and β_i^- are the charging and discharging rates of ES i, respectively; ξ_{it}^+ and ξ_{it}^- are the sets of non-negative slack variables to depict the outflow and injection imbalance of active power at node i during period t, respectively; ζ_{it}^+ and ζ_{it}^- are the non-negative slack variables that describe the outflow and injection imbalance of reactive power at node i, respectively; Ξ is the polyhedral uncertainty set for source-load power; $\boldsymbol{u}$, $\boldsymbol{y}^{\mathrm{b}}$, $\boldsymbol{y}^{\mathrm{c}}$, and $\boldsymbol{\xi}$ are the decision variable sets for the second stage Φ; u_{it}^{LD} and u_{it}^{PV} are the active load power and PV output at node i during period t, respectively; $z_{it}^{\mathrm{ES}+}$ and $z_{it}^{\mathrm{ES}-}$ are the charging and discharging states of ES i, respectively; $z_{it}^{\mathrm{GL}+}$ and $z_{it}^{\mathrm{GL}-}$ are the purchase and sell states of the grid-connected line (GL), respectively; Q_{it}^{PV} is the reactive power of PV i; $P_{it}^{\mathrm{ES}+}$ and $P_{it}^{\mathrm{ES}-}$ are the active charging and discharging power of ES i, respectively; Q_{it}^{ES} is the reactive power of ES i; S_{it} is the state of charge (SOC) for ES i; $P_{it}^{\mathrm{GL}+}$ and $P_{it}^{\mathrm{GL}-}$ are the purchased and sold active power of GL i, respectively; Q_{it}^{GL} is the reactive power of GL i; Q_{it}^{LD} is the reactive power, demand of load i; P_{ijt}, Q_{ijt}, and I_{ijt} are the active power, reactive power and squared current magnitude on line ij, respectively; V_{it} is the squared voltage magnitude at node i; and T and I are the numbers of periods and nodes, respectively.

Equation (1) details the objective of the total PV capacity and the first-stage variable set x. The constraints of the first-stage optimization are stated in (2). Specifically, the first sub-equation defines the configured ES capacity with an identified PV hosting capacity for the integrated PV-ES system at node i, and the second and third sub-equations describe the values of the maximal charging and discharging power corresponding to the capacity of ES i. Equation (3) presents the objective of the total power imbalance and the decision variable sets.

A. Uncertainty Set of Source-load Power

$$\Xi = \left\{ u_{it}^{\mathrm{PV}}, u_{it}^{\mathrm{LD}} \middle| \begin{array}{l} u_{it}^{\mathrm{LD}-} \le u_{it}^{\mathrm{LD}} \le u_{it}^{\mathrm{LD}+} \quad \forall i, \forall t \\ \Delta_i^{\mathrm{LD}-} \sum\limits_{t=1}^{T} u_{it}^{\mathrm{LD}*} \le \sum\limits_{t=1}^{T} u_{it}^{\mathrm{LD}} \le \Delta_i^{\mathrm{LD}+} \sum\limits_{t=1}^{T} u_{it}^{\mathrm{LD}*} \quad \forall i \\ C_i^{\mathrm{PV}} u_{it}^{\mathrm{PV}-} \le u_{it}^{\mathrm{PV}} \le C_i^{\mathrm{PV}} u_{it}^{\mathrm{PV}+} \quad \forall i, \forall t \\ \Delta_i^{\mathrm{PV}-} \sum\limits_{t=1}^{T} u_{it}^{\mathrm{PV}*} \le \sum\limits_{t=1}^{T} \dfrac{u_{it}^{\mathrm{PV}}}{C_i^{\mathrm{PV}}} \le \Delta_i^{\mathrm{PV}+} \sum\limits_{t=1}^{T} u_{it}^{\mathrm{PV}*} \quad \forall i \end{array} \right\} \tag{4}$$

where $[u_{it}^{\mathrm{LD}-}, u_{it}^{\mathrm{LD}+}]$ is the predicted interval of u_{it}^{LD}; $u_{it}^{\mathrm{LD}*}$ is

the predicted nominal value of u_{it}^{LD}; $[\Delta_i^{\mathrm{LD}-}, \Delta_i^{\mathrm{LD}+}]$ is the budget range of load uncertainty; $[u_{it}^{\mathrm{PV}-}, u_{it}^{\mathrm{PV}+}]$ and $u_{it}^{\mathrm{PV}*}$ are the predicted interval and the nominal PV output per unit capacity, respectively; and $[\Delta_i^{\mathrm{PV}-}, \Delta_i^{\mathrm{PV}+}]$ is the budget range of PV uncertainty.

Constraint (4) expresses the detailed polyhedral uncertainty set for source-load power. The first row limits the uncertainty of active load power within the predicted interval, and the second line controls the degree of load uncertainty, i.e., the total deviation between the uncertainty power u_{it}^{LD} and the predicted nominal value $u_{it}^{\mathrm{LD}*}$ throughout the whole horizon does not exceed the budget range. The third and fourth rows indicate the uncertainty of PV active power, which has similar meanings as the first and second rows. It can be observed that u_{it}^{PV} demonstrates DDU associated with the first-stage variable C_i^{PV}.

B. Constraints for Energy Storages

$$z_{it}^{\mathrm{ES}+} + z_{it}^{\mathrm{ES}-} \le 1 \quad \forall i, \forall t \tag{5}$$

$$\begin{cases} 0 \le P_{it}^{\mathrm{ES}+} \le M_i^{\mathrm{ES}+} z_{it}^{\mathrm{ES}+} \\ 0 \le P_{it}^{\mathrm{ES}-} \le M_i^{\mathrm{ES}-} z_{it}^{\mathrm{ES}-} \end{cases} \quad \forall i, \forall t \tag{6}$$

$$-\left(P_{it}^{\mathrm{ES}+} + P_{it}^{\mathrm{ES}-} \right) \tan\left(\cos^{-1} pf_i^{\mathrm{ES, min}} \right) \le Q_{it}^{\mathrm{ES}} \le$$
$$\left(P_{it}^{\mathrm{ES}+} + P_{it}^{\mathrm{ES}-} \right) \tan\left(\cos^{-1} pf_i^{\mathrm{ES, min}} \right) \quad \forall i, \forall t \tag{7}$$

$$S_{it} = S_{i(t-1)} + P_{it}^{\mathrm{ES}+} \Delta t \eta_i^{\mathrm{ch}} - P_{it}^{\mathrm{ES}-} \Delta t / \eta_i^{\mathrm{dis}} \quad \forall i, \forall t \tag{8}$$

$$\begin{cases} S_i^{\min} C_i^{\mathrm{ES}} \le S_{it} \le S_i^{\max} C_i^{\mathrm{ES}} \\ S_{iT} = S_{i0} = 0.5 C_i^{\mathrm{ES}} \end{cases} \quad \forall i, \forall t \tag{9}$$

where $M_i^{\mathrm{ES}+}$ and $M_i^{\mathrm{ES}-}$ are the maximum allowable charging and discharging power of ES i, respectively; $pf_i^{\mathrm{ES, min}}$ is the minimum power factor for ES operation; η_i^{ch} and η_i^{dis} are the charging and discharging efficiencies, respectively; $[S_i^{\min}, S_i^{\max}]$ is the proportional range of SOC for ES i; and S_{iT} and S_{i0} are the final and initial SOC of ES i, respectively.

The scheduling constraints under uncertainty are illustrated in (5)-(19). Specifically, (5) restricts the charging and discharging states of ES i during period t, i.e., the ES cannot be charged and discharged simultaneously. This ensures the optimality and rationality of the operating state of the ES for the non-convex TSRO model [7]. Constraint (6) ensures that the active charging power and discharging power of ES i are not higher than the maximal allowable power. This constraint contains bilinear terms which can be linearized via the Big-M method. Constraint (7) further limits the reactive power of ES i. Constraint (8) expresses the temporal evolution of the SOC for ES i. Constraint (9) shows that the SOC of ES i should be within the proportional range during every period [8]. Besides, the final SOC should be restored to its initial value, thereby providing a stable initial SOC of the ES for the next scheduling horizon.

C. Constraints for Grid-connected Lines

$$z_{it}^{\mathrm{GL}+} + z_{it}^{\mathrm{GL}-} \le 1 \quad \forall i, \forall t \tag{10}$$

$$\begin{cases} 0 \le P_{it}^{\mathrm{GL}+} \le M_i^{\mathrm{GL}+} z_{it}^{\mathrm{GL}+} \\ 0 \le P_{it}^{\mathrm{GL}-} \le M_i^{\mathrm{GL}-} z_{it}^{\mathrm{GL}-} \end{cases} \quad \forall i, \forall t \tag{11}$$

$$\left\| P_{it}^{GL+} \quad P_{it}^{GL-} \quad Q_{it}^{GL} \right\|_2 \le M_i^{GL} \quad \forall i, \forall t \tag{12}$$

where M_i^{GL+} and M_i^{GL-} are the maximal allowable purchase and sell power of GL i, respectively; and M_i^{GL} is the maximal capacity of GL i. Equation (10) constrains the purchase and sell states of the GL at node i during period t, i.e., the GL cannot purchase and sell power at the same time during any period. Constraint (11) guarantees that the active purchase and sell power of GL i does not exceed its maximal allowable power. After considering the reactive power of the GL, the second-order cone relaxation (SOCR) constraint (12) maintains that its apparent power does not exceed the maximal capacity.

D. Constraints for Renewable and Load Units

$$-u_{it}^{PV} \tan\left(\cos^{-1} pf_i^{PV,\min}\right) \le Q_{it}^{PV} \le u_{it}^{PV} \tan\left(\cos^{-1} pf_i^{PV,\min}\right) \quad \forall i, \forall t \tag{13}$$

$$Q_{it}^{LD} = u_{it}^{LD} \tan\left(\cos^{-1} pf_i^{LD}\right) \quad \forall i, \forall t \tag{14}$$

where $pf_i^{PV,\min}$ is the minimal power factor for PV i; and pf_i^{LD} is the constant power factor for load i.

The PV reactive power at node i is limited in (13). Equation (14) denotes the reactive power demand of load i. PVs and loads are considered as uncontrollable units in the scheduling.

E. Constraints for Power Systems

$$u_{it}^{PV} - u_{it}^{LD} + P_{it}^{ES-} - P_{it}^{ES+} + P_{it}^{GL+} - P_{it}^{GL-} + \xi_{it}^+ = $$
$$\xi_{it}^- + \sum_{j \in \vartheta(i)} P_{ijt} - \sum_{s \in \ell(i)} \left(P_{sit} - r_{si} I_{sit}\right) \quad \forall i, \forall t \tag{15}$$

$$Q_{it}^{PV} - Q_{it}^{LD} + Q_{it}^{ES} + Q_{it}^{GL} + \zeta_{it}^+ = $$
$$\zeta_{it}^- + \sum_{j \in \vartheta(i)} Q_{ijt} - \sum_{s \in \ell(i)} \left(Q_{sit} - x_{si} I_{sit}\right) \quad \forall i, \forall t \tag{16}$$

$$V_{jt} = V_{it} - 2\left(r_{ij} P_{ijt} + x_{ij} Q_{ijt}\right) + \left(r_{ij}^2 + x_{ij}^2\right) I_{ijt} \quad \forall ij, \forall t \tag{17}$$

$$\left\| 2P_{ijt} \quad 2Q_{ijt} \quad I_{ijt} - V_{it} \right\|_2 \le I_{ijt} + V_{it} \quad \forall ij, \forall t \tag{18}$$

$$\begin{cases} \left(V_i^{\min}\right)^2 \le V_{it} \le \left(V_i^{\max}\right)^2 & \forall i \\ 0 \le I_{ijt} \le \left(I_{ij}^{\max}\right)^2 & \forall ij, \forall t \end{cases} \tag{19}$$

where r_{ij} and x_{ij} are the resistance and reactance of line ij, respectively; $\vartheta(i)$ and $\ell(i)$ are the line sets with node i as parent and child nodes, respectively; $V_i^{\min}$ and $V_i^{\max}$ are the minimal and maximal voltage magnitudes at node i, respectively; and $I_{ij}^{\max}$ is the maximal current capacity of line ij; P_{sit}, Q_{sit}, and I_{sit} are the active power, reactive power, and squared current magnitude on line si, respectively; and r_{si} and x_{si} are the resistance and reactance of line si, respectively.

Constraints (15)-(19) support the DistFlow model for power networks in the formulation of SOCR. Specifically, (15) and (16) govern the active and reactive power balance at node i, respectively. For instance, if there is net active power inflow of node i during period t, $\xi_{it}^- > 0$, $\xi_{it}^+ = 0$; otherwise, if there is net active power outflow, $\xi_{it}^+ > 0$, $\xi_{it}^- = 0$. Equation (17) calculates the voltage drop on line ij with Ohm's law. The power capacity of line ij is bounded by (18) after

SOCR, and (19) further maintains the security of nodal voltage and line current.

III. SOLUTION ALGORITHM

For ease of algorithmic demonstration, the DDU-based TSRO model formulated in Section II is abbreviated into the following compact model M_1.

$$\begin{cases} M_1: \max_{x} A^T x \\ \text{s.t.} \quad Cx \le b \\ \quad \Phi = \max_{u \in \Xi} \min_{y^b \in \{0,1\}, y^c, \xi} 1^T \xi \\ \quad \text{s.t.} \quad \Xi = \left\{ u \,\middle|\, \underline{F}x + \underline{d} \le u \le \bar{F}x + \bar{d} \right\} \\ \quad Gy^b + Hy^c + \begin{bmatrix} 1 & -1 \end{bmatrix} \xi \le f - Jx - Ku \\ \quad \left\| Ly^c \right\|_2 \le my^c + n \end{cases} \tag{20}$$

where the objectives and constraints are described in matrices. Apart from the decision variables in each stage defined in Section II, the other matrices (A, C, b, $\underline{F}$, $\underline{d}$, $\bar{F}$, $\bar{d}$, G, H, f, J, K, L, m, and n) in M_1 are constants with appropriate dimensions. It can be observed that the uncertainty variables u in M_1 are affected by the first-stage variables x, and this model features DDU and binary recourses. As different optimal results of x in the first stage shake the feasible region of u, i.e., the uncertainty set Ξ is changing during the iterative solution, the classic nested column and constraint generation (C&CG) algorithm will encounter the issues of oscillation and non-convergence. To overcome this weakness, a normalization scheme is exploited to equate M_1 into a regular TSRO model.

Proposition: M_1 can be normalized as the following regular TSRO model M_2.

$$\begin{cases} M_2: \max_{x} A^T x \\ \text{s.t.} \quad Cx \le b \\ \quad \Phi' = \max_{u' \in \Xi'} \min_{y^b \in \{0,1\}, y^c, \xi} 1^T \xi \\ \quad \text{s.t.} \quad \Xi' = \left\{ u' \,\middle|\, 0 \le u' \le 1 \right\} \\ \quad Gy^b + Hy^c + \begin{bmatrix} 1 & -1 \end{bmatrix} \xi \le f - Jx - \\ \qquad K\left(\underline{F}x + \underline{d} + u' \circ \left(\bar{F}x + \bar{d} - \underline{F}x - \underline{d} \right) \right) \\ \quad \left\| Ly^c \right\|_2 \le my^c + n \end{cases} \tag{21}$$

where $\circ$ denotes the Hadamard product of vectors. In M_2, Ξ' is no longer affected by the first-stage variables x, and u' is the DIU [9]. Hence, M_2 is a regular TSRO model.

Proof: to prove the above proposition, we only need to prove the following two claims.

1) Claim 1: for $\forall u \in \Xi$, there always exists $u' \in \Xi'$ such that $\underline{F}x + \underline{d} + u' \circ \left(\bar{F}x + \bar{d} - \underline{F}x - \underline{d} \right) = u$.

2) Claim 2: for $\forall u' \in \Xi'$, $\underline{F}x + \underline{d} + u' \circ \left(\bar{F}x + \bar{d} - \underline{F}x - \underline{d} \right) \in \Xi$ always holds.

For Claim 1, if $\bar{F}x + \bar{d} - \underline{F}x - \underline{d} = 0$, then u' can take any value within [0, 1]; if $\bar{F}x + \bar{d} - \underline{F}x - \underline{d} > 0$, then $0 \le u' \le 1$. Claim 1 is proven.

For Claim 2, for $\forall u' \in [0, 1]$, we always have $\underline{F}x + \underline{d} \le$

$\underline{F}x + \underline{d} + u' \circ (\bar{F}x + \bar{d} - \underline{F}x - \underline{d}) \leq \bar{F}x + \bar{d}$. Claim 2 is proven.

Based on Claim 1 and Claim 2, Ku in M_1 is replaced by $K(\underline{F}x + \underline{d} + u' \circ (\bar{F}x + \bar{d} - \underline{F}x - \underline{d}))$, then Ξ can be directly extended to Ξ'. In this case, M_1 is equivalent to M_2.

M_2 is a regular TSRO problem with binary recourses, which can be directly handled using the classic nested C&CG algorithm. This algorithm uses an outer C&CG procedure to decouple M_2 into an iterative master-slave problem framework. The slave problem is further converted into an iterative problem containing the inner-loop master and slave problems via an inner C&CG procedure [10]. The optimal results are finally derived by nested iterative computations.

A. Slave Problem

Substituting the optimal results $\tilde{x}$ from the master problem, the slave problem is then formulated as SP.

$$
\begin{cases}
\text{SP: } \max_{u' \in \Xi'} \min_{y^b \in \{0,1\}, y^c, \xi} \mathbf{1}^T \xi \\
\text{s.t. } \Xi' = \{u \mid 0 \leq u' \leq 1\} \\
\quad Gy^b + Hy^c + \begin{bmatrix} 1 & -1 \end{bmatrix} \xi \leq f - J\tilde{x} - \\
\quad\quad K(\underline{F}\tilde{x} + \underline{d} + u' \circ (\bar{F}\tilde{x} + \bar{d} - \underline{F}\tilde{x} - \underline{d})) \\
\quad \|Ly^c\|_2 \leq my^c + n
\end{cases} \tag{22}
$$

As y^b indicates binary recourse variables, SP cannot be mathematically merged as one single-level max model by duality. It is further decomposed to an inner-loop slave and master iterative problems [11], and the specific formulations are detailed as follows.

1) Inner-loop Slave Problem

Substituting the kth iterative results u'_k from the inner-loop master problem, the inner-loop slave is written as ISP.

$$
\begin{cases}
\text{ISP: } \phi = \min_{y^b \in \{0,1\}, y^c, \xi} \mathbf{1}^T \xi \\
\text{s.t. } Gy^b + Hy^c + \begin{bmatrix} 1 & -1 \end{bmatrix} \xi \leq f - J\tilde{x} - \\
\quad\quad K(\underline{F}\tilde{x} + \underline{d} + u'_k \circ (\bar{F}\tilde{x} + \bar{d} - \underline{F}\tilde{x} - \underline{d})) \\
\quad \|Ly^c\|_2 \leq my^c + n
\end{cases} \tag{23}
$$

The optimal results $(y^b_{k+1}, y^c_{k+1}, \xi_{k+1})$ are fed back to the inner-loop master problem.

2) Inner-loop Master Problem

After substituting y^b_{k+1} optimized by ISP, the inner-loop master problem is defined as IMP.

$$
\begin{cases}
\text{IMP: } \varphi = \max_{u' \in \Xi', \eta, \alpha, \beta^1_\vartheta, \beta^2_\vartheta} \eta \\
\text{s.t. } \Xi' = \{u \mid 0 \leq u' \leq 1\} \\
\quad \eta \leq \alpha^T \{ f - J\tilde{x} - Gy^b_{k+1} - K[\underline{F}\tilde{x} + \underline{d} + \\
\quad\quad u' \circ (\bar{F}\tilde{x} + \bar{d} - \underline{F}\tilde{x} - \underline{d})] \} - \sum_{\forall \vartheta} n^T_\vartheta \beta^2_\vartheta \\
\quad \|\beta^1_\vartheta\|_2 \leq \beta^2_\vartheta \\
\quad H^T \alpha + \sum_{\forall \vartheta} (L^T_\vartheta \beta^1_\vartheta + m^T_\vartheta \beta^2_\vartheta) = 0 \\
\quad -1 \leq \alpha \leq 0 \\
\quad \beta^2_\vartheta \geq 0 \quad \forall \vartheta, \forall k
\end{cases} \tag{24}
$$

where η is an auxiliary variable to characterize the objective function; α is the dual variable corresponding to the first constraint on y^c in ISP; β^1_ϑ and β^2_ϑ are the dual variables of the SOCR constraints on y^c in ISP; ϑ is the dimension of the SOCR constraints [12]; and u' is the collection of extreme points of Ξ', as the uncertainty set Ξ' is a polytope, which corresponds to binary variables.

The bilinear term $\alpha^T u'$ is linearized using the Big-M method [13], and IMP is equivalent to a mixed-integer second-order cone programming (MISOCP) problem. The optimal u'_{k+1} is passed to ISP for the next iteration until the convergent solution $(\tilde{u}', \tilde{y}^c, \tilde{y}^b)$ of SP is obtained.

B. Master Problem

The master problem is cast as MP after plugging the solution results $\tilde{u}'$ from SP as $\tilde{u}'_j$.

$$
\begin{cases}
\text{MP: } \max_{x, y^b_l, y^c_l} A^T x \\
\text{s.t. } Cx \leq b \\
\quad Gy^b_l + Hy^c_l \leq f - Jx - \\
\quad\quad K[\underline{F}x + \underline{d} + \tilde{u}'_l \circ (\bar{F}x + \bar{d} - \underline{F}x - \underline{d})] \\
\quad \|Ly^c_l\|_2 \leq my^c_l + n \quad 1 \leq l \leq j
\end{cases} \tag{25}
$$

where j is the iteration number of MP and SP, and the two problems are iteratively solved until convergence. The procedures of the nested C&CG algorithm for tackling a regular TSRO model with binary recourses can be referred to [14].

IV. NUMERICAL EXPERIMENTS

To verify the effectiveness and superiority of the proposed approach, numerical experiments are implemented for a microgrid and a distribution network on four typical days. The tested microgrid is a practical 0.4 kV system in Singapore. PV and ES systems are integrated at node 4 with certain capacities, and the topology and basic operation parameters of this microgrid are given in Fig. 1 and Table I, respectively. The investigated distribution network is the IEEE 123-node system with a voltage base of 4.16 kV. The PV and ES systems are integrated at nodes 33, 67, 86, 97, 116, and 123, and the system parameters are available in [15].
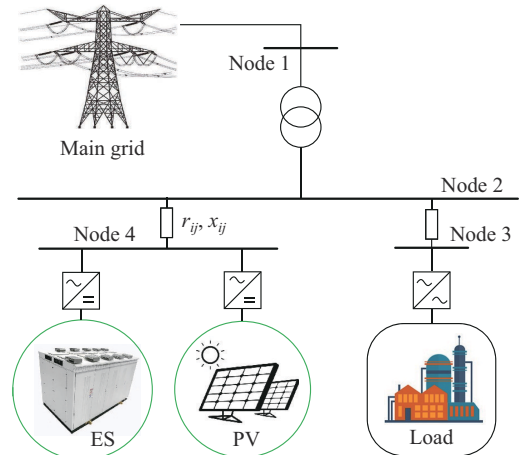

Fig. 1.　Topology of tested microgrid.

The 24-hour scheduling horizon is divided into 48 periods. Therefore, the optimization model totally contains 4×48 periods. The predicted nominal active power of PV under unit hosting capacity (1 kW) of the four days under the Singapore environment is depicted in Fig. 2, and the predicted error of PV generation is ±15% of the nominal value. Besides, the predicted nominal curves of active load power for the typical days are also displayed in Fig. 2, and its predicted error is ±5%. The nodal load profiles of the IEEE 123-node system are scaled with their load capacities. For both tested systems, α_i is defined as 0.2, and $\beta_i^+ = \beta_i^- = 0.5$.

TABLE I
BASIC OPERATION PARAMETERS OF TESTED MICROGRID

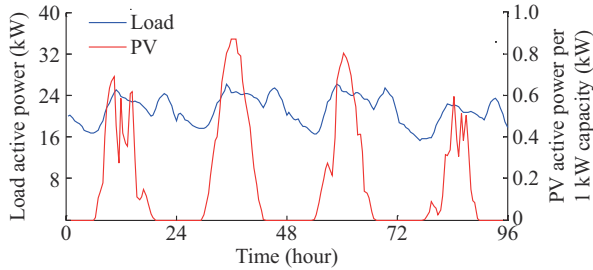| Parameter	Value	Parameter	Value
α_i	0.2	I	4
β_i^+, β_i^-	0.5	T	48
$\Delta_i^{PV-}, \Delta_i^{PV+}$ (%)	92, 108	Δt (min)	30
$\Delta_i^{LD-}, \Delta_i^{LD+}$ (%)	98.5, 101.5	pf_i^{LD}	0.85
$\eta_i^{ch}, \eta_i^{dis}$	0.98, 0.98	r_{12}, x_{12} (Ω)	0.25, 0.083
S_i^{min}, S_i^{max}	0.2, 0.95	r_{23}, x_{23} (Ω)	0.23, 0.075
M_i^{GL+}, M_i^{GL-} (kW)	25, 10	r_{24}, x_{24} (Ω)	0.18, 0.058
M_i^{GL} (kVA)	30	V_i^{min}, V_i^{max} (p.u.)	1.05, 0.95
$pf_i^{ES,min}, pf_i^{PV,min}$	0.98, 0.98	I_{ij}^{max} (A)	120

Fig. 2. Predicted nominal PV and load active power on four typical days.

Multiple cases are also set for comparative analysis. Specifically, Case 1 is the proposed approach, Case 2 denotes the classic nested C&CG algorithm [14], and Case 3 expresses the adaptive algorithm in [6]. The strong duality is adopted for constraint generation. All numerical simulations are performed on a 64-bit laptop with a 2.30 GHz CPU and 8 GB RAM, and the optimization is modeled and solved by MATLAB-R2018b calling YALMIP package and CPLEX-12.8 solver. The optimal results of all cases are reported in Table II.

TABLE II
OPTIMAL RESULTS OF ALL CASES

Case	Microgrid			Distribution network		
	PV hosting capacity (kW)	Outer-loop iteration	Total solution time (s)	PV hosting capacity (kW)	Outer-loop iteration	Total solution time (s)
1	38.6	4	25.2	7.252	5	43.4
2		Oscillation	Non-convergence		Oscillation	Non-convergence
3	38.6	9	368.5	7.252	14	1693.8

According to Table II, for both systems, Case 1 converges after several outer-loop iterations, and the total solution time does not exceed 50 s. Case 2 directly resorts to the classic nested C&CG algorithm to address the TSRO problem with DDU, leading the iterative solution to jump back and forth among DDU. The phenomenon of oscillation occurs in Case 2, and the optimization cannot converge. The optimal objective of PV hosting capacity in Case 3 is almost the same as that in Case 1, indicating the optimality of the proposed approach. However, the total solution time of Case 3 is over ten times that in Case 1 because two slave problems are formulated in Case 3 for iterative computations. In addition, the enlargement of system size inevitably leads to the increase of solution time to a certain extent. For Cases 1 and 3, the total solution time increases by 172% and 459% from the microgrid to the distribution network, respectively. The computational performance of the proposed approach indicates its strong scalability.

V. CONCLUSION

This letter proposes a TSRO approach based on DDU to deal with the assessment problem of PV hosting capacity in power grids. The proposed approach efficiently overcomes the drawbacks of iterative oscillation and non-convergence in the classic algorithm under the influence of DDU, and considerably enhances the computational efficiency of such a complicated model. The proposed approach can be extended to a series of robust planning and scheduling problems containing DDU. It should be pointed that the non-anticipative issue in power system scheduling is not considered in this letter, as in other two-stage optimization studies; therefore, multi-stage RO approach with sequential DDU should be further investigated in future work.

REFERENCES

[1] L. Cheng, H. Zang, A. Trivedi *et al.*, "Mitigating the impact of photovoltaic power ramps on intraday economic dispatch using reinforcement forecasting," *IEEE Transactions on Sustainable Energy*, vol. 15, no. 1, pp. 3-12, Jan. 2024.

[2] P. Li, Z. Wu, C. Zhang *et al.*, "Multi-timescale affinely adjustable robust reactive power dispatch of distribution networks integrated with high penetration of PV," *Journal of Modern Power Systems and Clean Energy*, vol. 11, no. 1, pp. 324-334, Jan. 2023.

[3] L. Zhang, H. Ye, F. Ding *et al.*, "Increasing PV hosting capacity with an adjustable hybrid power flow model," *IEEE Transactions on Sustainable Energy*, vol. 14, no. 1, pp. 409-422, Jan. 2023.

[4] H. Wu, Y. Yuan, X. Zhang *et al.*, "Robust comprehensive PV hosting capacity assessment model for active distribution networks with spatiotemporal correlation," *Applied Energy*, vol. 323, p. 119558, Oct. 2022.

[5] S. Zhang, Y. Fang, H. Zhang *et al.*, "Maximum hosting capacity of photovoltaic generation in SOP-based power distribution network integrated with electric vehicles," *IEEE Transactions on Industrial Informatics*, vol. 18, no. 11, pp. 8213-8224, Nov. 2022.

[6] Y. Chen and W. Wei, "Robust generation dispatch with strategic renewable power curtailment and decision-dependent uncertainty," *IEEE Transactions on Power Systems*, vol. 38, no. 5, pp. 4640-4654, Sept. 2023.

[7] J. M. Arroyo, L. Baringo, A. Baringo *et al.*, "On the use of a convex model for bulk storage in MIP-based power system operation and planning," *IEEE Transactions on Power Systems*, vol. 35, no. 6, pp. 4964-4967, Nov. 2020.

[8] S. Singh, V. B. Pamshetti, A. K. Thakur *et al.*, "Profit maximization in ADN through voltage control and DR management with networked community micro-grids," *IEEE Transactions on Industry Applications*, vol. 59, no. 3, pp. 2706-2719, May-Jun. 2023.

[9] B. Zeng and W. Wang. (2022, Mar.). Two-stage robust optimization with decision dependent uncertainty. [Online]. Available: http://arxiv. org/abs/2203.16484

[10] X. Zheng, B. Zhou, X. Wang *et al.*, "Day-ahead network-constrained unit commitment considering distributional robustness and intraday discreteness: a sparse solution approach," *Journal of Modern Power Systems and Clean Energy*, vol. 11, no. 2, pp. 489-501, Mar. 2023.

[11] X. Cao, T. Cao, Z. Xu *et al.*, "Resilience constrained scheduling of mobile emergency resources in electricity-hydrogen distribution network," *IEEE Transactions on Sustainable Energy*, vol. 14, no. 2, pp. 1269-1284, Apr. 2023.

[12] L. Ma, L. Wang, and Z. Liu, "Soft open points-assisted resilience enhancement of power distribution networks against cyber risks," *IEEE Transactions on Power Systems*, vol. 38, no. 1, pp. 31-41, Jan. 2023.

[13] H. Qiu, W. Gu, W. Sheng *et al.*, "Resilience-oriented multistage scheduling for power grids considering nonanticipativity under tropical cyclones," *IEEE Transactions on Power Systems*, vol. 38, no. 4, pp. 3254-3267, Jul. 2023.

[14] L. Zhao and B. Zeng. (2012, Jan.). An exact algorithm for two-stage robust optimization with mixed integer recourse problems. [Online]. Available: https://optimization-online.org/2012/01/3310/

[15] X. Chen, W. Wu, B. Zhang *et al.*, "Data-driven DG capacity assessment method for active distribution networks," *IEEE Transactions on Power Systems*, vol. 32, no. 5, pp. 3946-3957, Sept. 2017.

Haifeng Qiu received the B. Eng. degree from Nanjing Normal University, Nanjing, China, in 2015, and the Ph. D. degree from Southeast University, Nanjing, China, in 2021, both in electrical engineering. From 2019 to 2020, he was a Visiting Scholar with Cornell University, Ithaca, USA. He is currently a Postdoctoral Research Fellow with the School of Electrical and Electronic Engineering, Nanyang Technological University, Singapore. His research interests include energy system planning, operation, and market trading.

Veerapandiyan Veerasamy received the B. Eng. degree in electrical and electronic engineering from Anna University, Chennai, India, in 2013, and the Ph. D. degree from University Putra Malaysia, Serdang, Malaysia, in 2022. He is currently working as a Postdoctoral Research Fellow with the School of Electrical and Electronic Engineering, Nanyang Technological University, Singapore. His research interests include robust controller, recurrent neural network, and power flow analysis.

Chao Ning received the B. Eng. degree in automation from University of Electronic Science and Technology of China, Chengdu, China, in 2012, the M. S. degree in control science and engineering from Tsinghua University, Beijing, China, in 2015, and the Ph.D. degree from Cornell University, Ithaca, USA, in 2020. He is currently working as Assistant Professor with the Department of Automation, Shanghai Jiao Tong University, Shanghai, China. His research interests include data-driven optimization under uncertainty, learning-based model predictive control, artificial intelligence, energy process system engineering, power system operation, and hydrogen energy system.

Qirun Sun received the B.Eng. degree in electrical engineering from Southeast University, Nanjing, China, in 2018, where he is pursuing the Ph.D. degree. He is currently a Visiting Scholar with the School of Electrical and Electronic Engineering, Nanyang Technological University, Singapore. His research interests include resilient planning and operation of multi-carrier energy system.

Hoay Beng Gooi received the B.S. degree from National Taiwan University, Taipei, China, in 1978, the M. S. degree from the University of New Brunswick, Fredericton, Canada, in 1980, and the Ph.D. degree from Ohio State University, Columbus, USA, in 1983, all in electrical engineering. He was an Assistant Professor with Lafayette College, Easton, USA, during 1983-1985, and a Senior Engineer with the Control Data-Energy Management System Division, Plymouth, USA, for about six years before joining Nanyang Technological University (NTU), Singapore, in 1991. He is an Associate Professor with the School of Electrical and Electronic Engineering. Since 2020, he has been the Co-director of SP Group-NTU Joint Lab. His current research interests include microgrid energy management system dealing with energy storage, condition monitoring, electricity market, and spinning reserve.